Electronic structure and magnetic properties of Ni$_{1-x}$Mn$_x$Al alloys

V. REDNIC[a,b*], O. ISNARD[c], M. NEUMANN[d], L. REDNIC[a,b], M. COLDEA[a], N. ALDEA[b]

[a]*Babes-Bolyai University, Faculty of Physics, Kogalniceanu 1, 400084 Cluj-Napoca, Romania*
[b]*National Institute for Research and Development of Isotopic and Molecular Technologies, P. O. Box 700, 400293 Cluj-Napoca, Romania*
[c]*Université J. Fourier, Institut Néel du CNRS, 25 rue des martyrs, 38042 Grenoble Cedex 9, France*
[d]*University of Osnabrück, Fachbereich Physik, 49069 Osnabrück, Germany*

XPS, magnetization and magnetic susceptibility measurements of Ni$_{1-x}$Mn$_x$Al (x=0.0, 0.2, 0.3, 0.4, 0.5, 0.6, 0.8) alloys are reported. X-ray diffraction measurements showed that all investigated alloys are single phases with the same CsCl structure type. The hybridization between Al 3sp and Ni 3d states and Al 3sp and Mn 3d states leads to a partial filling of the Ni and Mn 3d bands. Like in the parent compound NiAl, the Anderson condition for the existence of a local magnetic moment on Ni site in   Ni$_{1-x}$Mn$_x$Al is not fulfilled. The contribution of Ni atoms to the measured magnetic susceptibility may be explained in the frame of the self-consistent renormalization theory of spin fluctuations. The ferromagnetic behaviour of the Ni$_{1-x}$Mn$_x$Al alloys (x>0) is due to the interaction of local magnetic moments confined on Mn sites. The correlation between the magnetic results in the ordered and paramagnetic state indicates the presence of a number of antiferromagnetically coupled Mn-Mn pairs.

1. Introduction

The problem of local moments confined to the transition metals (T) sites, i.e., localized behaviour in some aspects of itinerant electrons, is one of the most important issues in the physics of the magnetic alloys and intermetallic compounds [1].

The correlation between the experimental magnetic data and XPS spectra leads to a better understanding of the magnetic properties of d-band alloys and intermetallic compounds, because the density of states at Fermi level and the XPS valence band spectrum in these metallic systems is dominated by d – electron contribution [2].

The compound NiAl crystallizes in the CsCl (B2) structure type with a = 2.87 Å, is a Pauli paramagnet and the electronic structure calculations indicated that the Ni 3d band is completely filled [3]. On the other hand, the XPS studies have shown that the Ni 3d electrons in this compound are located in the area of the flat sp-band of the Al host and form a narrow resonance (virtual bound state) at about 2 eV binding energy [4]. This result suggests that the Ni 3d band in NiAl is not completely filled and that the magnetic properties of this compound should be explained in the frame of the spin-fluctuation model [5]**.**

From the point of view of the itinerant electron system, the Ni 3d band in NiAl is partially unoccupied, but the binding energies of the spin-up and spin-down states do not differ too much, and the ordered magnetic moment can be negligible.

The metastable alloy phase τ - MnAl with a L1$_0$ structure type may be described as a tetragonal distorted B$_2$ – structure type with the lattice parameters a = b = 2.77 Å and c = 3.57Å. It is observed only near the composition Mn$_{1.11}$Al$_{0.89}$ and from magnetization measurements was obtained a mean magnetic moment of μ^{exp}_{Mn} = 2.0μ_B [6]. The excess Mn atoms situated in the Al sublattice are coupled antiferromagnetically to the Mn sublattice. The band structure calculation of hypothetical MnAl (with B$_2$ structure type) showed that the d-band is partially filled with the Fermi energy E$_F$ at a peak in the density of states N(E) [7]. For the theoretical magnetic moment of the hypothetical MnAl was obtained the value μ^{th}_{Mn} = (1.8 to 2.0) μ_B [7] which agree with the experimental one.

Magnetic properties of the Ni$_{1-x}$Mn$_x$Al alloys in the ordered magnetic state were reported in literature [8], but there are no explanation regarding the relatively small values of the measured magnetic moments on transition metal atoms, their variation with Ni concentration and if Ni atoms have a contribution to the measured magnetic susceptibility.

The aim of this paper is to explain the magnetic properties of the investigated alloys by correlating the magnetic measurements, in the ordered and paramagnetic state, with XRD and XPS results.

2. Experimental

Seven samples from the $Ni_{1-x}Mn_xAl$ system (x=0.0, 0.2, 0.3, 0.4, 0.5, 0.6, 0.8) were prepared by argon arc melting method. The samples were melted repeatedly, at least four times, in the same atmosphere to ensure homogeneity. The weight loss of the final furnace-cooled samples was found to be less than 1%. The purity of starting materials was 99.999% for Al and 99.99% for Mn and Ni. XRD measurements were performed on polished surfaces using a Bruker D8 Advance diffractometer, due to the hardness of the samples.

The XPS spectra were recorded using a PHI 5600ci ESCA spectrometer with monochromatized Al K_α radiation at room temperature. The pressure in the ultra-high vacuum chamber was in the 10^{-10} mbar range during the measurements. The samples were cleaved in situ. The surface cleanness was checked by monitoring the O 1s and C 1s core levels in the survey spectra. Their intensity was very low, indicating a negligible contamination.

The magnetic measurements were performed using a vibrating sample magnetometer (VSM) in the temperature range 4 K - 500 K and fields up to 10T. The variation of the magnetic susceptibility with the temperature was obtained using a Weiss balance in the 300 K - 750 K temperature range.

3. Results and discussion

3.1 XRD measurements

X-ray diffraction patterns are presented in Fig.1. The broad character of the peaks indicates the presence of the strains in the samples. All the investigated alloys are single phases with the same CsCl (B2) structure type, confirming the earlier findings. The lattice parameter, estimated using the Powder Cell program, increases monotonically with Mn concentration from a=2.875 Å for NiAl to a=2.966 Å for $Ni_{0.2}Mn_{0.8}Al$ and is given in the last column of Table 1.
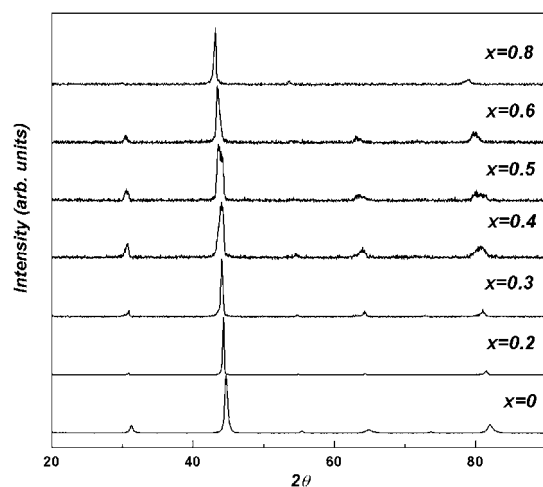

Fig. 1. X-ray diffraction pattern of $Ni_{1-x}Mn_xAl$ alloys.

3.2 XPS measurements

The XPS valence band spectra of NiAl (Fig. 2) shows a narrow resonance at about 2 eV superposed on the Al 3sp states, confirming the earlier findings [4]. The shoulder near Fermi level is due to the Al 3sp states. The XPS valence band spectra of $Ni_{1-x}Mn_xAl$ alloys are similar to that of the parent compound NiAl, but a difference can be clearly observed, namely, the line-width of the valence band increases with the Mn content. This is due to the Mn 3d states, which are concentrated at the bottom of the valence band in the 2.5-3eV binding energy region, as previously demonstrated by band structure calculation and experimental measurements for many alloys and intermetallic compounds based on Mn [9-11].
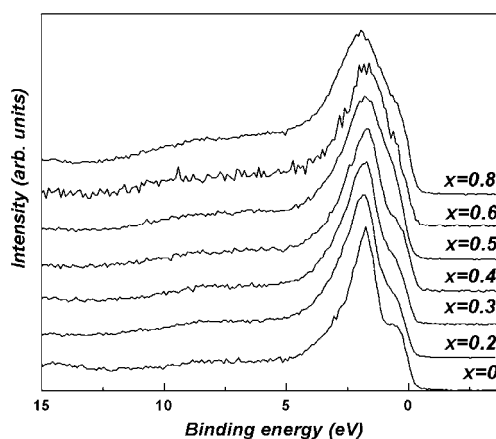

Fig. 2. The XPS valence band spectra of $Ni_{1-x}Mn_xAl$ alloys.

There is also an appreciable hybridization between the Mn 3d and Al 3sp states which leads to a partial filling of the Mn 3d band. Each Mn atom is surrounded by eight Al atoms at distances of about 2.57 Å. These data indicate that there is no formation of a common d-band in $Ni_{1-x}Mn_xAl$ alloys, thus confirming the validity of the rigid band model for the electronic structure of such alloys and intermetallic compounds. As a consequence, in all these alloys Ni atoms do not carry any magnetic moments in measured magnetization.

The Ni 2p spectra for all investigated alloys are situated at the same binding energy BE, but are shifted to higher BE relative to pure metallic Ni (Fig .3). This also confirms the partial filling of Ni 3d band in the $Ni_{1-x}Mn_xAl$ alloys. The first vicinity of Ni atoms in the $Ni_{1-x}Mn_xAl$ alloys does not change by alloying, what explains the lack of the chemical shift in the Ni 2p spectra. In Ni metal the Ni 2p satellite structure, situated at about 6.5 eV higher BE energy, is an evidence for unoccupied 3d states. If there exists a small amount of unoccupied Ni 3d states, like in $Ni_{1-x}Mn_xAl$ alloys, a d-electron may be transferred via the hybridization when one adds photohole to the Ni 2p orbital. It may lead to the formation of the weak satellite structures (Fig. 3). This is not the 6 eV satellite in Ni metal, but a kind of transfer satellite [2]. For high Mn concentrations the feature around 852 eV corresponds to the Mn Auger line $L_3M_{45}M_{45}$.
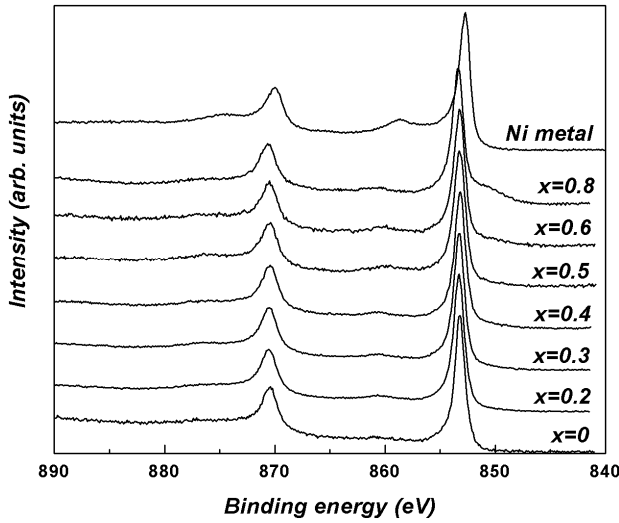
Fig. 3. Ni 2p XPS spectra of $Ni_{1-x}Mn_xAl$ alloys and pure metallic Ni.

The Mn 3s core level spectra show an exchange splitting around 4 eV arising from the exchange interactions between the core hole and the open 3d shell. This is a direct evidence of the local magnetic moments on Mn sites. The exchange splitting in MnNi is about 5.2 eV and the Mn magnetic moment is about 4 μ_B/Mn [12]. The exchange splitting is proportional with the Mn local moment [2]. Fig. 4 presents the curve fitting results of $Mn_{0.8}Ni_{0.2}Al$ alloy, after background subtraction, and the similar spectrum of MnNi compound [13].
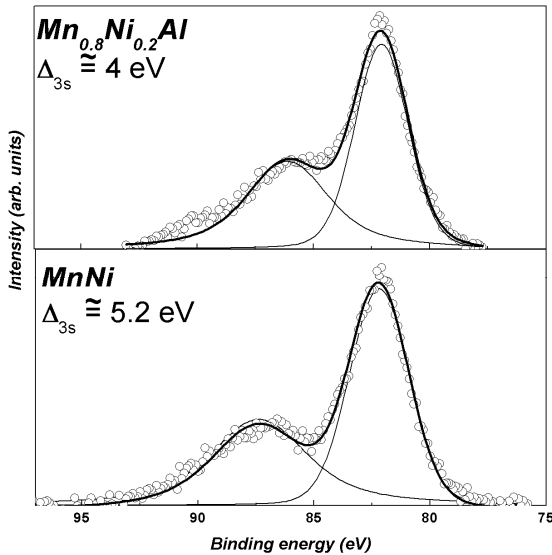

Fig. 4. Mn 3s curve fitting results of $Mn_{0.8}Ni_{0.2}Al$ alloy and MnNi compound.

3.3 Magnetic measurements

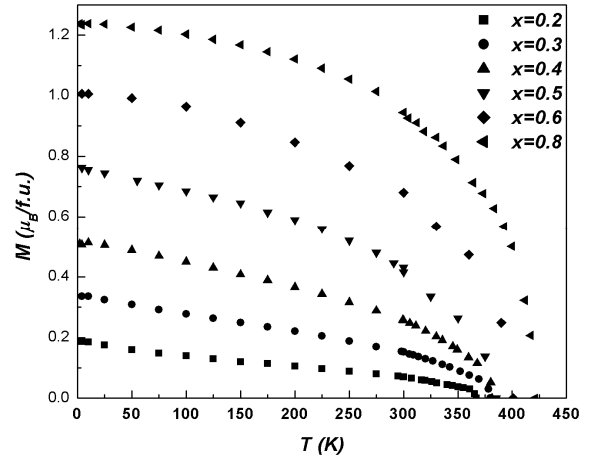The temperature dependence of the spontaneous magnetization of $Ni_{1-x}Mn_xAl$ alloys is shown in Fig. 5.

Fig. 5. Temperature dependence of spontaneous magnetization of $Ni_{1-x}Mn_xAl$ alloys.

The values and variations of magnetization with magnetic field (Fig. 6) and temperature suggest that all the investigated alloys have a ferromagnetic behaviour, below the corresponding Curie temperatures.
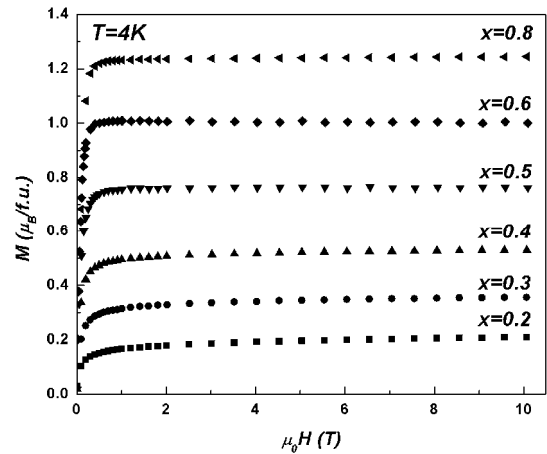

Fig. 6. Magnetic field dependence of magnetization at T=4K of $Ni_{1-x}Mn_xAl$ alloys.

The Curie temperatures T_C have been determined in the molecular field approximation from the linear dependence of $M_{FM}^2(T)$ in the region around T_C. The values of the magnetic moments and T_C are given in Table 1. The measured Mn magnetic moments are in good agreement with the values determined earlier by Hara et al [8].

The thermal variation of the reciprocal magnetic susceptibility for the investigated alloys in the high temperature range is shown in Fig. 7.

The experimental data fit a Curie-Weiss law with a small additional temperature-independent term χ_0, in which the principal contribution is brought by the Pauli susceptibility χ_P of the conduction electrons:
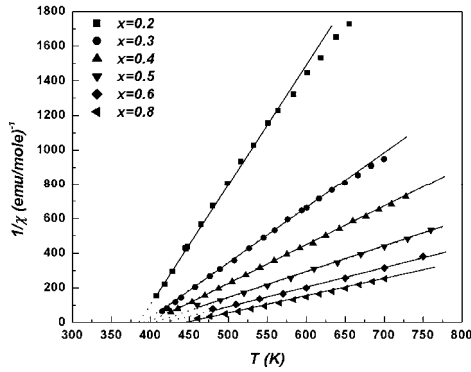
$$\chi=C/(T-\theta) + \chi_0$$

Fig. 7. Reciprocal susceptibility versus temperature of $Ni_{1-x}Mn_xAl$ alloys.

Table 1. The magnetic moments in the ordered μ and paramagnetic state μ_{eff}, the Curie T_C and paramagnetic Curie θ temperatures and the lattice constants a of the $Ni_{1-x}Mn_xAl$ alloys.

	μ (μ_B/f.u.)	μ_{eff} (μ_B/f.u.)	T_C (K)	θ (K)	a (Å)
x=0					2.8752
x=0.2	0.19	1.06	367	385.7	2.8919
x=0.3	0.34	1.57	379.8	395	2.906
x=0.4	0.51	1.9	381.5	398.8	2.9155
x=0.5	0.77	2.32	385	405.5	2.927
x=0.6	1.01	2.66	401	422.7	2.9356
x=0.8	1.24	2.9	420.8	445.9	2.9664

As was expected, the contribution of the χ_0 term in the measured magnetic susceptibility is more pronounced for small Mn concentrations, and is observed as a deviation from the linearity of the reciprocal susceptibility in the high temperature region.

The magnetic susceptibility of NiAl does not depend on temperature in the (80-300)K range and has the value $\chi_{NiAl}^{meas} = 22.7 \times 10^{-6}$ emu/mol [14], arising from three contributions $\chi_{NiAl}^{meas} = \chi_P + \chi_L + \chi_{dia}$, where χ_P is the Pauli susceptibility of the conduction electrons, χ_L is the Landau diamagnetism of the conduction electrons and χ_{dia} is the diamagnetism of the atomic cores. The Pauli susceptibility in the free electron approximation is given by $\chi_P^0 = 1.86 \times 10^{-6}(M / \rho)^{2/3} n^{1/3}$ emu/mol [15], where M is the molar mass, ρ the density and n is the number of s, p and d valence electrons per unit formula. For NiAl, $\chi_P^0 = 25 \times 10^{-6}$ emu/mol and the Landau diamagnetism $\chi_L = -1/3 \chi_P^0 = - 8.33 \times 10^{-6}$ emu/mol. The diamagnetic contribution to the measured susceptibility has the value $\chi_{dia} = \chi_{dia}^{Al} + \chi_{dia}^{Ni} = -15.5 \times 10^{-6}$ emu/mol [14]. These values give rise to an enhanced Pauli susceptibility $\chi_P = 46.54 \times 10^{-6}$ emu/mol. The Stoner enhancement factor f $= \chi_P / \chi_P^0 = 1.86$ shows that NiAl in an exchange - enhanced Pauli paramagnet. This result suggests that the $Ni_{1-x}Mn_xAl$ alloys are also exchange – enhanced Pauli paramagnets, which are correctly treated in the self-consistent renormalization theory of spin fluctuations [5]. This theory has revealed that only a small - q part of the wave number-dependent susceptibility χ_q contributes to the temperature dependence of χ in the exchange - enhanced Pauli paramagnets. The average amplitude of the local spin fluctuations $< S_L^2 > = 3 k_B T \Sigma_q \chi_q$ on Ni sites increases with temperature until it reaches an upper limit determined by the charge neutrality condition. The temperature dependence of χ at low temperatures is the result of the increase of local moments with increasing temperature. The amplitude of thermally excited longitudinal spin fluctuations saturates at certain temperature T* above which the susceptibility is governed by local moment type fluctuations and therefore a Curie-Weiss behavior is observed, so that in the high temperature range the Ni atoms contribute also to the measured magnetic susceptibility.

The correlation of the magnetic data from both ordered and paramagnetic states confirms this assumption.

The values of the effective magnetic moments μ_{eff} and the paramagnetic Curie temperatures θ are also given in Table 1.

The Curie temperatures T_C and θ increase monotonically with Mn concentration in good agreement with the theory of ferromagnetic materials, T_C being proportional with the number Z of neighboring magnetic atoms. Indeed, since the magnetic moment of Ni atoms in the ordered state can be neglected, the measured magnetic moments may be attributed to Mn atoms only. The values of the Mn spins were obtained from the relation $\mu_{Mn} = 2 S_{Mn}\mu_B$ and are given in Table 2, together with the theoretical values of the Mn effective magnetic moments given by $\mu_{eff}^{Mn} = 2\sqrt{S_{Mn}(S_{Mn}+1)}\mu_B$. One can notice that in such high symmetry crystal lattice, the local environment plays in favour of a reduced and probably negligible orbital moment, thus justifying the above equation for the ordered moment. This calculated values per unit formula are smaller than those experimentally determined, therefore in the paramagnetic region one have to consider the contribution of Ni magnetic moments induced by temperature activated spin fluctuations, according to the relation $\mu(f.u.)_{eff}^2 = x(\mu_{eff}^{Mn})^2 + y(\mu_{eff}^{Ni})^2$, where x and y are the molar fractions of Mn and Ni, respectively. The Ni effective magnetic moment has reasonable value for $x \leq 0.4$, comparable with the values on Ni sites in other spin fluctuation systems [16, 17]. For x > 0.4, the calculated Ni effective magnetic moments are too large; this suggests that in the ordered magnetic state not all the Mn moments are coupled ferromagnetically, but there are some antiferromagnetic Mn-Mn pairs, as was also observed in many other Mn based alloys [13]. The probability for the existence of Mn-Mn antiferromagnetic pairs increases with Mn concentration.

Table 2. The magnetic moments and spin of Mn atoms estimated in the ordered state assuming a ferromagnetic coupling and the calculated Mn effective magnetic moment of the $Ni_{1-x}Mn_xAl$ alloys.

	μ_{ord}^{Mn}	S_{Mn}	μ_{eff}^{Mn}
x=0.2	0.95	0.48	1.69
x=0.3	1.13	0.57	1.89
x=0.4	1.28	0.64	2.05
x=0.5	1.54	0.77	2.33
x=0.6	1.68	0.84	2.49
x=0.8	1.55	0.78	2.36

The strong Mn 3d - Al 3sp hybridization is due to the high number of Al atoms in the Mn first vicinity, namely 8 Al atoms at ~2.5 Å. This explains the small values of the Mn magnetic moments in $Ni_{1-x}Mn_xAl$ alloys comparing to MnNi. The Mn magnetic moment in the ordered state increases with Mn concentration, except for the x=0.8 alloy. This variation can be associated with the increase of the lattice parameter which leads to a decreasing in the Mn 3d - Al 3sp hybridization degree.
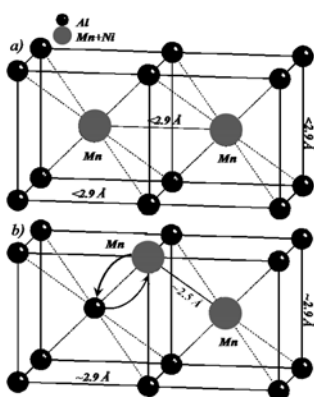

Fig. 8. Possible situations for Mn-Mn distance smaller than 2.9 Å.

But together with the Mn concentration, increases also the probability of the Mn-Mn antiferromagnetic pairs formation, so that a number of Mn magnetic moments do not contribute to the magnetization. These two phenomena influence the value of the measured magnetic moments. It is well known that Mn-Mn interaction is antiferromagnetic when the distance is smaller than ~2.9 Å [18], comparable with the lattice constant in $Ni_{1-x}Mn_xAl$ alloys. For larger values the coupling is ferromagnetic. In these alloys there are two possibilities for the appearance of antiferromagnetic Mn-Mn pairs:

• There are two Mn atoms in the centre of near neighbour cells and lattice parameter is smaller than 2.9 Å (Fig. 8 a);

• A crystallographic disorder appears: Mn and Al atoms switch places, thus the Mn-Mn distance became ~2.5 Å (Fig. 8 b).

4. Conclusions

The substitution of Ni for Mn in NiAl leads to no significant changes in the crystallographic structure, but has remarkable effects on the magnetic properties and electronic structure of $Ni_{1-x}Mn_xAl$ alloys. The investigated alloys present a ferromagnetic behaviour below the corresponding Curie temperatures. The Ni for Mn substitution leads to a progressive reduction of the ordered magnetization. Nevertheless the correlation between the results from ordered and paramagnetic state indicates the presence of some antiferromagnetically Mn-Mn pairs. The Ni 3d electrons form a narrow resonance (virtual bound states) superposed on the Al 3sp states. Ni 3d band is almost filled due to the hybridization with Al 3sp states, so

that the Anderson condition for the existence of a local moment on Ni sites in not fulfilled. The magnetic measurements in the high temperature range pointed out the existence of spin fluctuations on Ni sites in all investigated samples. The strong hybridization between Mn 3d and Al 3sp states is responsible for the lower values of the Mn magnetic moments.

References

[1] V. Yu. Irkhin, M. I. Katsnelson, A. V. Trefilov, J. Phys.: Cond. Matter. **5**, 8763 (1993).

[2] S. Hüfner, Photoelectron Spectroscopy Principles and Applications, Springer-Verlag, Berlin, 1995.

[3] Ch. Müller, H. Wonn, W. Blau, P. Ziesche, V. P. Krivitshii, Phys Stat Sol. B **95**, 215 (1979).

[4] P. Steiner, H. Höchst, W. Steffen, S. Hüfner, Z. Physik, **B 38**, 191 (1980).

[5] T. Moriya, Spin Fluctuation in Itinerant Electron Magnetism, Springer, New York, 1985.

[6] P. B. Braun, J. A. Goedkoop, Acta Cryst., **16**, 737 (1963).

[7] W. Blau, Ch. Müller, H. Wonn, Phys. Stat.Sol. A **59**, K203 (1980).

[8] Y. Hara, R. C. O' Handley, N. J. Grant, J. Magn. Magn. Mater. **54-57**, 1077 (1986).

[9] Y. Kurtulus, R. Dronskowski, J. Sol. State Chem. **176**, 390 (2003).

[10] R. Y. Umetsu, K. Fukamichi, A. Sakuma, J. Magn. Magn. Mat. **239**, 530 (2002).

[11] S. Plogmann, T. Schlatholter, J. Braun, M. Neumann, Yu. Yarmoshenko, M. V. Yabloskikh, E. I. Shreder, E. Z. Kurmaev, Phys. Rev. B **60**, 6428 (1999).

[12] L. Pál, E. Krén, G. Kádár, P. Szabó, T. Tarnóczi, J. Appl. Phys. **39**, 538 (1968).

[13] V. Rednic, M. Coldea, S. K. Mendiratta, M. Valente, V. Pop, M. Neumann, L. Rednic, J. Mag. Mag. Mat. **321**, 3415 (2009).

[14] M. B. Brodsky, J. O. Britain, J. Appl. Phys. **40**, 3615 (1969).

[15] M. Coldea, I. Pop, Phil. Mag., **28**, 881 (1973).

[16] M. Coldea, S. Chiuzbaian, M. Neumann, D. Todoran, M. Demeter, R. Tetean, V. Pop, Acta Phys. Pol. A **98**, 629 (2000).

[17] M. Coldea, V. Pop, L. G. Pascut, D. Todoran, Modern Physics Letter B **20**, 1 (2006).

[18] A. Kjekshus, R. Mollebud, A. F. Andresen, W. B. Pearson, Phil. Mag. **16**, 1063 (1967).

*Corresponding author: vrednic@itim-cj.ro